Collisional statistics of a stochastic single file

A. Taloni[1] and F. Marchesoni[1,2]
[1]*Dipartimento di Fisica, Università di Camerino, I-62032 Camerino, Italy*
[2]*Michigan Center for Theoretical Physics, University of Michigan, Ann Arbor, Michigan 48109-1120, USA*
(Received 16 August 2006; published 21 November 2006)

The anomalous diffusion of a single file of Brownian particles moving on a circle at a given temperature is characterized in terms of nearest-neighbor collisions. The time and the distance a particle diffuses (normally) between two successive collisions are computed numerically; their means, distributions, and correlation functions are determined for different values of the file parameters and reproduced analytically by means of simple phenomenological arguments. Most notably, the jump autocorrelation functions develop slow power-law tails. The ensuing impact representation of the single file dynamics suggests an alternate description of the single file diffusion as a geometrically constrained fluctuation mechanism.

DOI: 10.1103/PhysRevE.74.051119 PACS number(s): 05.40.Jc

I. INTRODUCTION

As the design and the operation of biology inspired nanodevices are becoming experimentally more and more accessible, understanding particle diffusion in one-dimensional (1D) systems has been recognized as a central issue in transport control [1]. A large category of such 1D devices is characterized by constrained flow geometries, where each particle is free to move, either ballistically or stochastically, between two neighbors which it cannot pass by any means. Inhibiting the particle hopping dramatically affects the diffusive nature of the resulting single file (SF) [2].

Here, we consider a file of N indistinguishable, unit-mass Brownian particles moving on a segment of length L; if the particle-particle interaction is hard-core (with zero radius), the elastic collisions between neighboring particles are "nonpassing"—meaning that the particles can be labeled according to an ordered (single-file) sequence. As a result the long-time diffusion of an individual particle gets strongly suppressed [3–5].

In the thermodynamic limit ($L,N\to\infty$ with constant density $\rho\equiv N/L$) the mean square displacement of each file particle can be written as

$$\langle \Delta x^2(t)\rangle = \frac{\langle|\Delta x(t)|\rangle}{\rho}, \tag{1}$$

with $\langle|\Delta x(t)|\rangle$ denoting the mean absolute displacement of a free particle. For a *ballistic* single file (bSF) of unperturbed propagating particles, clearly $\langle|\Delta x(t)|\rangle=\langle|\dot{x}|\rangle t$, where $\langle\cdots\rangle$ is the ensemble average taken over the initial file velocities, and therefore

$$\langle \Delta x^2(t)\rangle = \frac{\langle|\dot{x}|\rangle}{\rho} t. \tag{2}$$

A bSF particle diffuses apparently like a Brownian particle with normal diffusion coefficient $D=\langle|\dot{x}|\rangle/(2\rho)$.

For a *stochastic* single file (sSF) of Brownian particles with damping constant γ at temperature T, the equality $\langle|\Delta x(t)|\rangle=\sqrt{4D_0t/\pi}$ yields the anomalous diffusion law

$$\langle \Delta x^2(t)\rangle = 2\frac{F}{\rho}\sqrt{t}, \tag{3}$$

where the mobility factor $F=\sqrt{D_0/\pi}$ is related to the single-particle diffusion constant $D_0=kT/\gamma$, and $\langle\cdots\rangle$ involves an additional stochastic average [6]. The normal (2) and the subdiffusive (or SF) regime (3) have been detected both numerically [5,7] and experimentally [8,9].

In real systems, like molecules diffusing through nanotubes or zeolites, crossovers between bSF and sSF diffusion may occur depending on the chosen operating conditions. The modeling of such crossover mechanisms [10] is mostly based on the notion of free particle propagation between two subsequent collisions, or *jump*. On the other hand, resolving the jump length and duration of particles diffusing in constrained geometries is well within the reach of the present experimental techniques. The jump statistics of a single Brownian particle on 1D and 2D periodic substrates has been investigated for decades with regard to adsorbates on crystal surfaces [11], transport in superionic conductors [12], dispersion of particles in optical traps [13], to mention but a few. Of lately, advances in colloid technology [9,14] opened up the possibility of observing the jump statistics of a stationary assembly of "nonpassing" particles confined onto closed paths. For a diffusing SF the jump statistics is determined by the simultaneous effect of the substrate wells, acting like traps, and the interparticle collisions, which restrict the path length accessible to the individual file components.

In this paper we show that the subdiffusive dynamics of a sSF is fully characterized by the collisional statistics of its constituents. In Sec. II we numerically extract the jump statistics for a stationary sSF diffusing on a circle. For simplicity we ignore the effects due to the periodic structure of the underlying substrate [15]. We find that the jump duration τ and displacement σ are independent random observables, respectively, with mean $\langle\tau\rangle=(\rho\sqrt{kT})^{-1}$ and variance $\langle\sigma^2\rangle=2\sqrt{kT}/(\gamma\rho)$. Most remarkably, although $\langle\tau\rangle$ and $\langle\sigma^2\rangle$ are inversely proportional to the SF density, the ensuing jump statistics describes *locally* the stochastic trajectory of a single Brownian particle, as suggested by the verified identity $\langle\sigma^2\rangle=2D_0\langle\tau\rangle$ (Einstein's relation). However, on adding

up n consecutive jumps, in Sec. III we prove that the mean square displacement $x^2(n)$ of a sSF particle grows proportionally to $n^{1/2}$, as expected from Eq. (3). Finally, the autocorrelation functions of both the jump lengths and durations decay according to the power-laws $n^{-3/2}$ and $n^{-1/2}$, respectively, for $n \gg n_d = \gamma\langle\tau\rangle$. This leads us to conclude in Sec. IV that an appropriate impact representation of the SF trajectories provides indeed a self-consistent explanation of SF diffusion as a *collective* phenomenon [16].

II. JUMP STATISTICS

The simulation of a sSF on a circle of radius $L/(2\pi)$, i.e., a segment of length L, requires assigning each particle an independent Brownian dynamics modeled by a viscous force $-\gamma\dot{x}_i$ and a random force $\xi_i(t)$. Here, $x_i(t)$ denotes the coordinate of the ith particle; $\xi_i(t)$ represents a Gaussian stochastic process with zero mean and autocorrelation function $\langle\xi_i(t)\xi_j(0)\rangle = 2\gamma kT\delta_{i,j}\delta(t)$. The coupling of the diffusing particles with their environment is chosen so as to ensure that the SF eventually approaches an equilibrium state with temperature T, independent of the damping constant γ.

In our simulations each particle of coordinate x_i is assigned a random initial position, $x_i(0)$, and velocity, $\dot{x}_i(0)$; upon each *elastic* collision it exchanges velocity with either neighbors, x_{i-1} or x_{i+1}, without altering the file labeling. As a result, the file dynamics is represented by N intertwined Brownian trajectories on a cylinder, as shown in Fig. 1; each trajectory is centered at its starting point $x_i(0)$ and diffuses according to the normal diffusion law $\langle\Delta x_i^2(t)\rangle = 2D_0 t$ with $\Delta x_i(t) = x_i(t) - x_i(0)$ and $D_0 = kT/\gamma$. Any time two such trajectories cross one another (collision), the corresponding particles swap trajectory and keep diffusing along their new trajectories up to a next collision; the path followed by each particle between two subsequent collisions is termed here a *jump*. The jump statistics (i.e., of the jump length and duration) in an equilibrium sSF is the main focus of the present paper.

The sSF mean square displacement is defined by

$$\langle\Delta x^2(t)\rangle = \frac{1}{N}\sum_{i=1}^{N}\langle[x_i(t) - x_i(0)]^2\rangle_s, \tag{4}$$

with $\langle\cdots\rangle_s$ denoting the average taken over an appropriate number of independent stochastic realizations (typically 30). Such an additional average is required by the finite length L of the simulated file support. In order to avoid finite volume effects, the simulated Brownian trajectories cannot diffuse a distance larger than L; correspondingly, our simulation runs must be terminated after time intervals substantially shorter than $L^2/(8D_0)$, lest the normal diffusion of the file center of mass comes into play [17]. In a previous report [15] we showed that the simulated quantity (4) reproduces quite closely the predicted law (3) for SF diffusion in the thermodynamic limit.

The jump statistics of the sSF was gathered as illustrated in Fig. 1(a). We set the time origin $t=0$ after an adequate thermalization transient, and traced the jumping trajectory

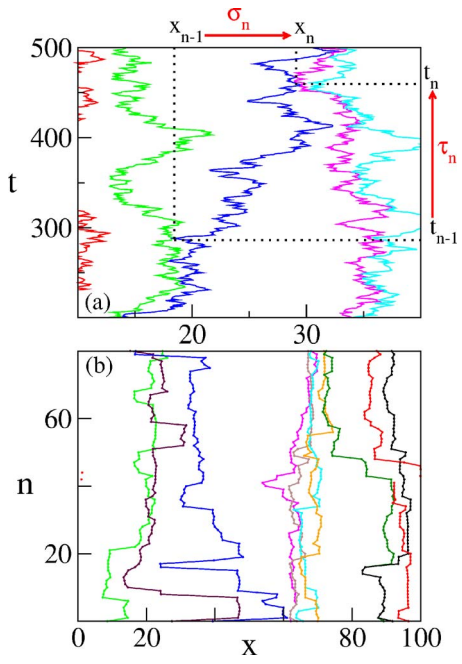

FIG. 1. (Color online) (a) Example of crossing trajectories for a sSF with $\gamma=5$, $kT=1$, and $\rho=0.1$ numerical simulation. The definition of $\tau_n^{(i)}$ and $\sigma_n^{(i)}$ for the (unlabeled) ith particle in the middle (blue curve) is illustrated for the reader's convenience. (b) Desynchronization transient $n=1-30$ in impact representation for a sSF with $N=10$ and all remaining simulation parameters as in (a). The impact order n is defined in the text; the periodic boundary conditions are apparent. Note that in this representation neighbor collisions do not correspond to trajectory crossings.

of, say, the ith particle until it underwent its nth collision at point $x_n^{(i)} = x_i(t_n^{(i)})$ and time $t_n^{(i)}$; the time interval $\tau_n^{(i)} = t_n^{(i)} - t_{n-1}^{(i)}$, with $t_0^{(i)} = 0$, denotes the duration of the nth jump of the ith particle; analogously, $\sigma_n^{(i)} = x_n^{(i)} - x_{n-1}^{(i)}$ defines the displacement associated with the jump and $|\sigma_n^{(i)}|$ is its length. Note that in elaborating the jump statistics we took *asynchronous* ensemble averages, i.e., we averaged over the jumps of all the N file particles according to their impact order, but regardless of their duration. Indeed, when two neighboring particles, i and $i+1$, collide at a given time t with $t \gg 0$, the condition $t_n^{(i)} = t_m^{(i+1)} = t$ holds (in general) for $n \neq m$ see Fig. 1(b) [18].

In Fig. 2 we focus on the temporal and spatial extension of the individual jumps. In panel (a) we display the variance σ_n^2 of the jump displacements versus the jump order n for different values of the file density ρ and the damping constant γ. In panel (b) the corresponding average time durations τ_n are plotted for the same values of the SF parameters as in (a). Two important properties are worth mentioning. (1) The jumps in a sSF are characterized by finite scales of length and duration, as suggested by the existence of the limits $\langle\tau\rangle = \lim_{n\to\infty}\tau_n$ and $\langle\sigma^2\rangle = \lim_{n\to\infty}\sigma_n^2$, respectively. (2) Both $\langle\sigma^2\rangle$ and $\langle\tau\rangle$ are inverse proportional to ρ, panels (c) and (d), thus implying that (1) is an effect of the constrained SF geometry. In this regard the sSF does not fit the continuous time random walk (CTRW) paradigm of subdiffusion [19]. Indeed, CTRW models assume that $\langle\tau\rangle$ and, possibly

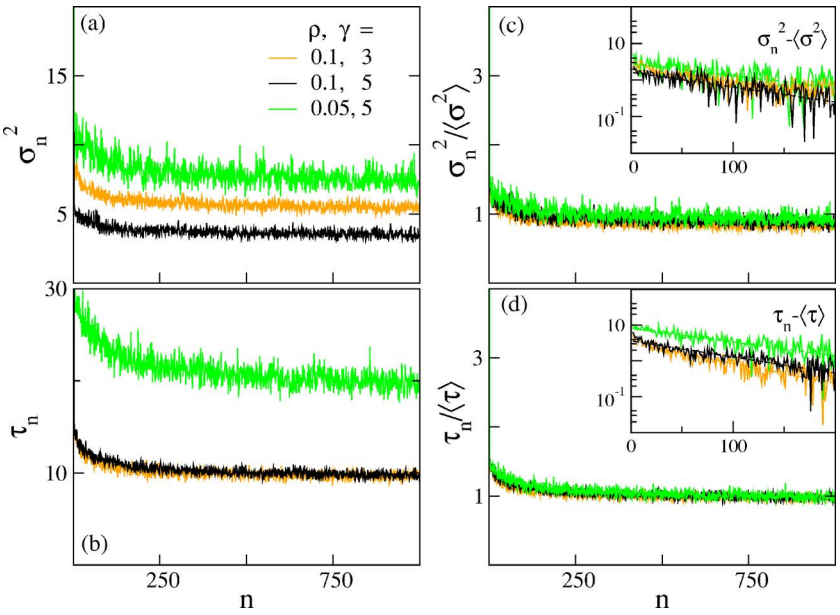

FIG. 2. (Color online) Jump statistics: (a) σ_n^2 vs n; (b) τ_n vs n, for the ρ and γ values reported in (a). The same quantities have been rescaled, respectively, in (c) and (d), for the sake of a comparison; the scaling parameters $\langle\sigma^2\rangle$, (10), and $\langle\tau\rangle$, (10), are both inverse proportional to ρ. Insets: exponential fits $\propto e^{-n/n^*}$ (dashed lines) of the corresponding decay branches $\sigma_n^2 \to \langle\sigma^2\rangle$ and $\tau_n \to \langle\tau\rangle$; in all cases the fitting parameter n^* falls within 10–20% of n_d in Eq. (12). Other simulation parameters are $kT=1$ and $N=5\times10^3$.

$\langle\sigma^2\rangle$, are infinitely large (or, rather, undefined) [20].

In Fig. 3 we re-interpret the subdiffusive properties of a sSF as a global collisional phenomenon. We recorded n consecutive jumps of the same particle after an initial transient of n_0 jumps, and computed the ensemble averages

$$x^2(n) = \left\langle \left(\sum_{k=1}^{n} \sigma_{n_0+k}^{(i)} \right)^2 \right\rangle, \tag{5}$$

$$t(n) = \left\langle \sum_{k=1}^{n} t_{n_0+k}^{(i)} \right\rangle. \tag{6}$$

The quantities (5) and (6), plotted respectively in panel (a) and (b) of Fig. 3, can be regarded as an impact representation of the continuous-time SF diffusion law (3). Indeed, it is apparent by inspection that: (3) Asymptotically, $t(n)$ grows linear in n, while $x^2(n)$ is proportional to $n^{1/2}$; both quantities scale with ρ and γ as implied by Eq. (3).

Finally, we investigated the statistical correlations of the jump lengths and durations by computing the stationary correlation functions

$$C_{\sigma,\sigma}(n) = \langle \sigma_{n_0}^{(i)} \sigma_{n_0+n}^{(i)} \rangle, \tag{7}$$

$$C_{\tau,\tau}(n) = \langle \tau_{n_0}^{(i)} \tau_{n_0+n}^{(i)} \rangle - \langle \tau_{n_0} \rangle^2, \tag{8}$$

$$C_{\tau,\sigma}(n) = \langle \tau_{n_0}^{(i)} \sigma_{n_0+n}^{(i)} \rangle, \quad C_{\sigma,\tau}(n) = \langle \sigma_{n_0}^{(i)} \tau_{n_0+n}^{(i)} \rangle, \tag{9}$$

with $n_0 \to \infty$, displayed in Fig. 4. The collisional mechanism is not memoryless: (4) The autocorrelation functions $C_{\sigma,\sigma}(n)$ of the jump displacement, shown in panel (a), do not vanish for $n>0$; in the limit $n \to 0$ they approach a small *negative*

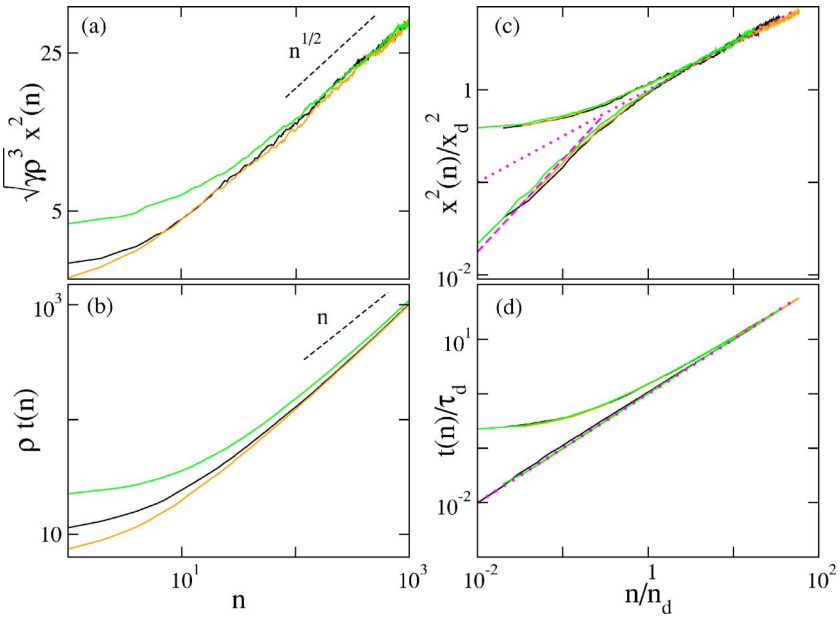

FIG. 3. (Color online) Anomalous diffusion: (a) $x^2(n)$ vs n; (b) $t(n)$ vs n, for $n_0=0$; ρ and γ are set as in Fig. 2. Both quantities have been rescaled for the sake of a comparison with Eq. (13); (c), (d) collapse of the numerical data for $x^2(n)$ and $t(n)$ on the universal curves (13) and (16) (dotted lines), respectively. Here, $x^2(n)$ and $t(n)$ have been computed also for $n_0=250$ (lower curve sets); short-time normal diffusion, with both $x^2(n)$ (dashed line) and $t(n)$ (dotted line) proportional to n, is hidden by the transient effects for $n_0=0$; it clearly emerges only for $n_0 \gtrsim n_d$. The asymptotic behavior sets in at $n=n_d$, regardless of the transient. Other simulation parameters are $kT=1$ and $N=5\times10^3$.

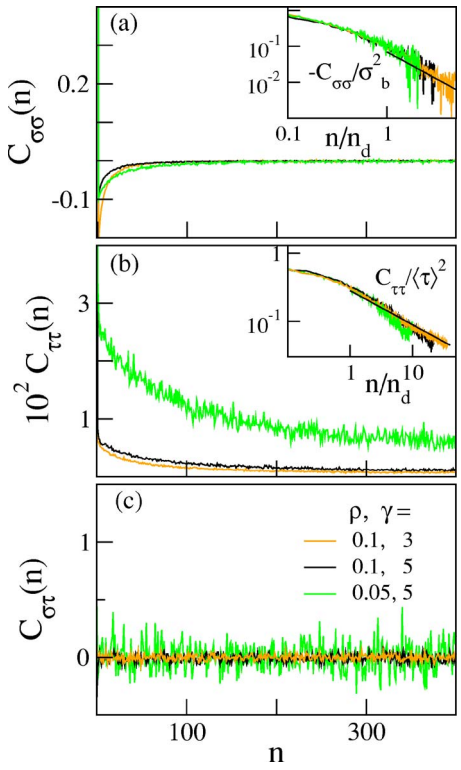

FIG. 4. (Color online) Jump correlations: (a) $C_{\sigma,\sigma}(n)$; (b) $C_{\tau,\tau}(n)$; (c) $C_{\sigma,\tau}(n)$ for the ρ and γ values reported in (c). Panel (a), inset: log-log plot of the negative $C_{\sigma,\sigma}(n)$ tails after appropriate rescaling; the solid line represents the power-law decay (25). The sum $\Sigma_{k=0}^{n} C_{\sigma,\sigma}(k)=0$ converges to zero proportionally to $n^{-1/2}$ (not shown). Panel (b): log-log plot of $C_{\tau,\tau}(n)/\langle\tau\rangle^2$ vs n/n_d; the solid line represents the asymptotic tail (27). Panel (c): $C_{\tau,\sigma}(n)$ is not reported as statistically indistinguishable from $C_{\sigma,\tau}(n)$. Other simulation parameters are $kT=1$ and $N=5\times10^3$.

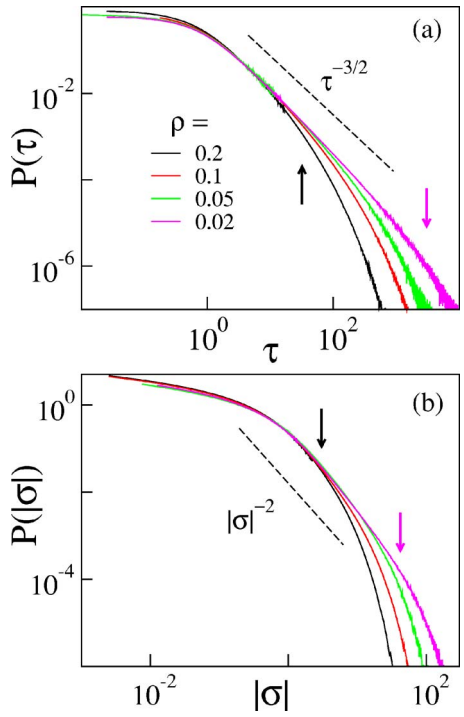

FIG. 5. (Color online) Jump duration and length densities: (a) $P(\tau)$; (b) $P(|\sigma|)$ for different densities ρ. The dashed lines represent the power laws $\tau^{-3/2}$ and $|\sigma|^{-2}$, respectively. On decreasing ρ, the knee of both distribution tails moves to higher values; vertical arrows in (a) and (b) point to τ_d and ρ^{-1}, respectively, for the extremal simulation densities (same color as for the relevant curves). Other simulation parameters are $kT=1$, $\gamma=3$, and $N=5\times10^3$.

value $C_{\sigma,\sigma}(0+)$, apparently insensitive to ρ, while, by definition, $C_{\sigma,\sigma}(0)=\langle\sigma^2\rangle>0$. The negative tail of $C_{\sigma,\sigma}(n)$ slowly decays to zero after an appropriate number of jumps, n_d, which is related to the time a single Brownian trajectory takes to diffuse a distance of the order ρ^{-1} [panel (a)]; (5) To a closer inspection, both autocorrelation functions (7) and (8) exhibit power-law tails for $n \gg n_d$, namely, $C_{\sigma,\sigma}(n) \propto -n^{-3/2}$ and $C_{\tau,\tau}(n) \propto n^{-1/2}$ [inset panels (a) and (b)]. The cross correlations $C_{\tau,\sigma}(n)$ and $C_{\sigma,\tau}(n)$ vanish at all n, because of the $\sigma \to -\sigma$ symmetry [panel (c)]. Note that properties (4) and (5), too, are incompatible with the current CTRW models, where each new jump is taken to be statistically independent of the preceding ones [19,20].

The following section is devoted to a phenomenological interpretation of our numerical simulations.

III. PHENOMENOLOGY OF THE COLLISIONAL MECHANISM

Properties (1)–(4) in Sec. II can be easily interpreted in terms of the standard theory of the free Brownian motion [21,22].

A. Jump distributions

First of all, we must explain why the collisional mechanism in a sSF is characterized by finite jumps. In order to determine $\langle\tau\rangle$ and $\langle\sigma^2\rangle$, i.e., the asymptotes of the curves in Fig. 2, we start from the densities of the jump durations, $P(\tau)$, and the jump lengths $|\sigma|$, $P(|\sigma|)$, both displayed in Fig. 5. Indeed, one can map the mutual collisions of two adjacent particles of coordinates $x_i(t)$ and $x_{i+1}(t)$ into the zero-crossings of the Brownian process defined by their relative distance $x_{i+1}(t)-x_i(t)$. As long as the trajectories of these two particles do not cross a third trajectory, the probability density for the time interval between two subsequent collisions to be τ is known to decay like $\tau^{-3/2}$ [22,23]. Moreover, the trajectory crossings of an isolated Brownian pair define a stochastic point process corresponding to a randomly sampled Wiener process with uncorrelated sampling time steps τ distributed according to the density $P(\tau)$; a simple calculation [22] leads to conclude that $P(|\sigma|)$ must be a Lorentzian function. Note that our simulation curves in Fig. 5(b) decay, indeed, like $|\sigma|^{-2}$.

This argument sure fails when the colliding pair interacts with another neighboring particle; these events are responsible for the knees in the tails of both $P(\tau)$ and $P(|\sigma|)$; as a consequence the measured $\langle\tau\rangle$ and $\langle\sigma^2\rangle$ are finite, properties (2) and (3). Notice that for $\rho \to 0$, i.e., in the absence of such knees, the densities $P(\tau)$ and $P(|\sigma|)$ would decay according to exact power laws with exponents $-3/2$ and -2, respectively. According to the standard CTRW scheme, however, the ensuing diffusion law would still be normal [20], as it should.

To a closer inspection, it is apparent that the power laws in Fig. 5 fail at both the short and the large scales. In particular, the $\tau^{-3/2}$ law for $P(\tau)$ is not tenable for times shorter than $\tau_b=\gamma^{-1}$, when the particles behave ballistically [21], and for times longer than $\tau_d=(D_0\rho^2)^{-1}$, when the adjacent file trajectory crossings cannot be neglected. We remark that for $t<\tau_b$ the Einstein relation $\langle x^2(t)\rangle=2D_0t$ does not apply at all, whereas τ_d has been estimated just by imposing

$$\langle [x_{i+1}(\tau_d)-x_i(\tau_d)]^2\rangle = 4D_0\tau_d = (2/\rho)^2.$$

A straightforward calculation for $\tau_d \gg \tau_b$ and $P(\tau)\propto\tau^{-3/2}$ yields

$$\langle\tau\rangle = \frac{\int_{\tau_b}^{\tau_d}\tau P(\tau)d\tau}{\int_{\tau_b}^{\tau_d}P(\tau)d\tau} = (\tau_b\tau_d)^{1/2} = \frac{1}{\rho\sqrt{kT}}. \tag{10}$$

Note that $\langle\tau\rangle$ is independent of γ as shown in Fig. 2(b). Moreover, recalling the definition of jump length, as the absolute displacement of an individual particle between two successive collisions, we conclude that recording the particle jumps corresponds to locally sampling the unperturbed Brownian trajectories, i.e., with no regard to possible trajectory crossings, so that $\langle\sigma^2\rangle=2D_0\langle\tau\rangle$. In view of our estimate (10) for $\langle\tau\rangle$ and ignoring finite damping terms $\mathcal{O}(kT/\gamma^2)$, we conclude that

$$\langle\sigma^2\rangle = \frac{2\sqrt{kT}}{\rho\gamma}. \tag{11}$$

[On including short-τ inertia effects [21], $\langle\sigma^2\rangle$ would slightly decrease as shown in Fig. 2(c),

$$\langle\sigma^2\rangle \to \langle\sigma^2\rangle[1-\tau_b/\langle\tau\rangle] = \langle\sigma^2\rangle - \sigma_b^2,$$

with $\langle\sigma^2\rangle$ given in Eq. (11) and $\sigma_b^2=2D_0\tau_b$. The correct value of $\langle\sigma^2\rangle$ is obtainable numerically from $P(\sigma)$.] Equations (10) and (11) provide a simple explanation of properties (1) and (2). Our estimate for $\langle\tau\rangle$ coincides with the time a ballistic particle with thermal speed $\sqrt{kT}$ takes to cross the mean interparticle distance ρ^{-1}. Of course, $\langle\tau\rangle$ is much shorter than τ_d, that is twice the time a particle takes to normally diffuse the same distance ρ^{-1}, $2D_0\tau_d=2/\rho^2\equiv\sigma_d^2$.

B. Subdiffusion in impact representation

As anticipated in the derivation of Eq. (11), we maintain that the local jump statistics of Figs. 2 and 5 is unfit to analyze a collective mechanism like the SF diffusion. (This remark holds true even if we already know that the upper bound to the jump size is inverse proportional to ρ; indeed, for two particles alone on a line, the jump size would diverge [22,23].) The SF geometry would come eventually into play only with the observation, property (4), that $C_{\sigma,\sigma}(n)$ and $C_{\tau,\tau}(n)$ in Fig. 4 decay to their asymptotic values for $n\to\infty$ after jump sequences of the order of

$$n_d = \frac{\tau_d}{\langle\tau\rangle} = \frac{\gamma}{\rho\sqrt{kT}}. \tag{12}$$

Alternate expressions for n_d, i.e.,

$$n_d = \frac{\langle\tau\rangle}{\tau_b} = \frac{\langle\sigma^2\rangle}{\sigma_b^2} = \frac{\sigma_d^2}{\langle\sigma^2\rangle},$$

follow immediately from the identities $\langle\sigma^2\rangle=(\sigma_b^2\sigma_d^2)^{1/2}$ and $\langle\tau\rangle=(\tau_b\tau_d)^{1/2}$.

Property (3), instead, provides the most natural connection between the local jump statistics with properties (1) and (2) and the many-body mechanism of SF diffusion (3). The linear growth of $t(n)$ with the length of the jump sequence n is a consequence of the existence of a finite mean collision time $\langle\tau\rangle$; indeed, the phenomenological relation

$$t(n) = \langle\tau\rangle n = \tau_d\frac{n}{n_d}, \tag{13}$$

fits well the curves of Fig. 3(b) for $n>n_d$, regardless of the actual impact time statistics.

Our analytical estimate for $x^2(n)$ is less straightforward. We started from de Gennes' theory of reptation of a polymer chain [24]

$$\langle x^2\rangle = \frac{1}{\rho}\langle|y|\rangle, \tag{14}$$

where $\langle x^2\rangle$ is the mean square displacement of a SF file particle and $\langle|y|\rangle$ is the displacement of an unperturbed Brownian trajectory, both at time t. As $y(t)$ is a Gaussian process, de Gennes' formula can be rewritten as

$$\langle x^2\rangle = \frac{1}{\rho}\sqrt{\frac{2}{\pi}\langle y^2\rangle}. \tag{15}$$

In impact representation, i.e., on replacing the continuous time t with the quantized time $t(n)$, and on making use of the central limit theorem, $\langle y^2\rangle\to\langle\sigma^2\rangle n$, Eq. (15) can be reformulated as

$$x^2(n) = \frac{2}{\rho}\sqrt{\frac{\langle\sigma^2\rangle}{2\pi}}n^{1/2} = x_d^2\left(\frac{n}{n_d}\right)^{1/2}, \tag{16}$$

with $x_d^2=\sigma_d^2/\sqrt{\pi}$. This formula fits well the asymptotic n dependence of the $x^2(n)$ curves in Fig. 3(a). The second identity (16) defines the universal scaling law plotted in Fig. 3(c). Therefore, Eqs. (13) and (16) provide a quantitative interpretation of property (3); moreover, if combined together, they satisfy the equality

$$x^2(n) = \frac{2}{\rho}\sqrt{\frac{D_0}{\pi}}t(n)^{1/2}, \tag{17}$$

which corresponds to an impact representation of the continuous time law (3). Steps (13)–(17) can thus be regarded as an alternate derivation of the SF diffusion law.

C. Transients in the jump statistics

The jump correlation functions plotted in Fig. 4 shed light onto the hidden dynamics of the SF collisional process, prop-

erty (4). Clearly, duration and length of the single jumps are statistically independent [see panel (c)]. More intriguing is the negative tail of $C_{\sigma,\sigma}(n)$ in panel (a). The correlation discontinuity at $n=0$, where $C_{\sigma,\sigma}(0)\simeq\langle\sigma^2\rangle$ and $C_{\sigma,\sigma}(0+)\lesssim 0$, can be explained by noticing that the jump displacements of two *isolated* overdamped Brownian particles coincide by definition; more importantly, for $\gamma\to\infty$ their sequence would amount to a randomly sampled zero-mean Wiener process; hence the expected identity $C_{\sigma,\sigma}(n>0)=0$. However, for finite damping constants, jumps with $\tau<\tau_b$ are the most frequent, as shown in Fig. 5(a), and ballistic in nature. This means that, as one particle encounters its partner, say, on the right, it bounces off to the left, so that a short jump to the right is likely to be followed by a jump to the left. Recalling that the characteristic length scale for the ballistic jumps of a Brownian pair is $\sqrt{2kT}/\gamma$, see discussion following Eq. (11), we conclude that

$$C_{\sigma,\sigma}(0+)=-\frac{2kT}{\gamma^2}=-\sigma_b^2. \tag{18}$$

Note that $C_{\sigma,\sigma}(0+)$ in Eq. (18) is independent of the particle density ρ, whereas the decay to zero of the negative $C_{\sigma,\sigma}(n)$ tails is controlled by the ρ-dependent diffusive scale n_d. Our data in Fig. 4(a) are seemingly well fitted by the exponential law $-\sigma_b^2 e^{-n/n_d}$ for $n\ll n_d$ (not shown), and by the power law $n^{-3/2}$ for $n\gg n_d$ [property (5)]. We checked that in the overdamped limit $\gamma\to\infty$, the negative tails become negligible with respect to $C_{\sigma,\sigma}(0)$.

We mentioned above on several occasions that τ_n, σ_n^2, $t(n)$, and $x^2(n)$ approach their asymptotic values only after a sufficiently long jump sequence. The decay of τ_n and σ_n^2 toward $\langle\tau\rangle$ and $\langle\sigma^2\rangle$, Fig. 2, is a mere transient effect. For $n=1$ these quantities are ensemble averages taken over the free paths between $t=0$ (simulation time origin) and the first recorded collision of each particle; these jumps are synchronized with respect to the particle impact order, though with different duration. The file (ensemble) particles have a fifty-fifty chance to collide with either neighbor, hence $\tau_1\simeq\tau_d/4$ and, from the Einstein's relation for $\gamma^2\ll kT\rho^2$, $\sigma_1^2\simeq(2\rho^2)^{-1}$. Both τ_1 and σ_1^2 are out of scale in Fig. 2; for a comparison, the reader is referred to Fig. 3, where definitions (5) and (6) with $n_0=0$ imply $\sigma_1^2=x^2(1)$ and $\tau_1=t(1)$.

For $n=2$ the averages are taken along the individual file trajectories in impact representation. The probability that a tagged particle executes its first two collisions with *different* neighbors is $(2n_d)^{-1}$, with $n_d\gg 1$, hence

$$\tau_2=\langle\tau\rangle\left(1-\frac{1}{2n_d}\right)+\frac{\tau_d}{2n_d}\simeq\frac{3}{2}\langle\tau\rangle$$

and, analogously, $\sigma_2^2\simeq(3/2)\langle\sigma^2\rangle$. These estimates for σ_2^2 and τ_2 reproduce well the $n\to 0+$ limit of the simulation curves plotted, respectively, in Figs. 2(c) and 2(d). For $n\gg n_d$, multiple trajectory crossings completely desynchronize the jumps in the averages of Fig. 2. This is the condition for the ergodic assumption to apply, hence our stationary estimates (10) and (11) for the impact parameters $\langle\tau\rangle$ and $\langle\sigma^2\rangle$.

The transient regime of the extensive quantities $x^2(n)$ and $t(n)$ is over for $n\gg n_d$, compare panels (a) and (b) of Fig. 3, regardless of the order n_0 of the starting jump. For $n_0=0$ the transient is dominated by the nonstationary desynchronization mechanism described above [see Fig. 1(b)], i.e., $\sigma_1^2=x^2(1)$ and $\tau_1=t(1)$. For n_0 of the order of, or larger than n_d, a stationary diffusion crossover becomes apparent: Initially, all Brownian particles start diffusing normally and independently of each other; after n_d additional jumps, they eventually perceive the presence of their file neighbors, therefore, the total jump mean square displacement $x^2(n)$ increases first proportional to n for $n\ll n_d$, $x^2(n)=\langle\sigma^2\rangle n$, and then proportional to $n^{1/2}$, as expected in the SF diffusion regime, for $n\gg n_d$. Most remarkably, Eq. (13) applies over the entire range of n with $n>1$, thus implying that after full desynchronization, the mean jump duration $\langle\tau\rangle$ is the same for both diffusive regimes, i.e., for $t>\tau_b$ [Fig. 3(d)].

The decay of $C_{\tau,\tau}(n)$ in Fig. 4(b) is a stationary process (i.e., independent of the file preparation at $t=0$) with a single particle switching partner in average every n_d jumps (see midtrajectory in Fig. 1). As a consequence, the exponential decay law, $C_{\tau,\tau}(n>0)\simeq\langle\tau\rangle^2 e^{-n/n_d}$, agrees well with the simulation data for $n\ll n_d$. [$C_{\tau,\tau}(0+)=\langle\tau\rangle^2$ should not be mistaken for $C_{\tau,\tau}(0)$, which, in view of the argument leading to Eq. (10), is proportional to $\langle\tau\rangle\tau_d$.] For $n\gg n_d$ the curves $C_{\tau,\tau}(n)$ develop intriguing slow tails, apparently decaying like $n^{-1/2}$ [Fig. 4(b), inset].

In conclusion, the stationary decays of $C_{\sigma,\sigma}(n)$ and $C_{\tau,\tau}(n)$ provide additional evidence for the geometric mechanism responsible for the subdiffusive dynamics (1.3): Both autocorrelation functions vanish only after jump sequences long enough to allow for multiple trajectory crossings. The physical meaning of the power-law decay of the jump autocorrelation functions, property (5), will be discussed in the forthcoming section.

IV. CONCLUSIONS

We studied the collisional dynamics of a stochastic single file (sSF) with particular emphasis on the mechanism responsible for its anomalous diffusion. By simulating the individual particle trajectories we determined the particle jump statistics, i.e., the statistics of the spatiotemporal separation between two subsequent collisions of the same particle, both at the local and the collective scales. Locally, the jump distributions can be interpreted in terms of the Brownian motion of a free colliding particle pair, the mean length and duration of the jumps being related to the mean distance of a neighbor pair in the SF. On a global scale, multiple trajectory crossings dominate the statistics of the jump sequences; de Gennes' reptation law allowed us to reproduce the subdiffusive dynamics of the sSF. In both limits the existence of finite spatiotemporal jump scales is connected to the finite mean interparticle distance (the inverse of the SF density), a parameter that quantifies the geometric restriction exerted on the free diffusion of the file constituents.

We now reformulate the key analytical results of Sec. III in a more compact notation. On rescaling $t\to\tilde{t}=\gamma t$ and

$x \to \tilde{x} = \rho x$, with $\rho = N/L$, the dynamics of the sSF turns out to be controlled by two parameters, only, namely,

$$kT \to Q = \left(\frac{\rho}{\gamma}\right)^2 kT, \tag{19}$$

$$L \to \tilde{L} = N. \tag{20}$$

In the thermodynamic limit, $N \to \infty$,

$$n_d = \tilde{n}_d = \frac{1}{\sqrt{Q}}, \tag{21}$$

so that from Eqs. (10) and (11)

$$\langle \tau \rangle \to \langle \tilde{\tau} \rangle = \frac{1}{\sqrt{Q}} = n_d, \tag{22}$$

$$\langle \sigma^2 \rangle \to \langle \tilde{\sigma}^2 \rangle = 2\sqrt{Q} = \frac{2}{n_d}, \tag{23}$$

valid for $Q \ll 1$. Moreover, $\tilde{\sigma}_d^2 = 2$, $\tilde{\tau}_d = 1/Q$, $\tilde{\sigma}_b^2 = 2Q$, and $\tilde{\tau}_b = 1$. The dimensionless formulation (19)–(23) is consistent with the rescaling of the numerical data adopted in Figs. 2–4. In particular, all universal curves discussed in Sec. 3 can be obtained by means of the rescaling rule: $t \to \tilde{t} = \gamma t$, $x \to \tilde{x} = \rho x$, and $n \to n/n_d$.

Finally, we comment on the physical implications of property (5). The tails of both $C_{\sigma,\sigma}(n)$ and $C_{\tau,\tau}(n)$ in Fig. 4 clearly cross over from an exponential to a power-law decay at around $n \sim n_d$. Even if an analytical explanation of such crossovers proved elusive, still we could show that the underlying mechanism is closely connected with the onset of the SF diffusion [16]. By definition, in the stationary regime

$$x^2(n) = \sum_{q,k=0}^{n} \langle \sigma_q \sigma_k \rangle = 2 \sum_{k=1}^{n-1} (n-k) \tilde{C}_{\sigma,\sigma}(k),$$

where for convenience we have introduced the symmetrized autorrelation function $\tilde{C}_{\sigma\sigma}(n) \equiv C_{\sigma\sigma}(n) - \frac{1}{2}\delta_{0,n}\langle \sigma^2 \rangle$. The asymptotic result (16) can be recovered only under two simultaneous conditions, namely,

$$\sum_{k=0}^{\infty} \tilde{C}_{\sigma,\sigma}(k) = 0 \tag{24}$$

and

$$C_{\sigma,\sigma}(n) \simeq -\frac{\sigma_b^2}{4\sqrt{\pi}} \left(\frac{n_d}{n}\right)^{3/2}, \tag{25}$$

both verified by the simulation data in Fig. 4(a). Finally, the alternate expression

$$x^2(n) \simeq \frac{\langle \sigma^2 \rangle}{\langle \tau \rangle^2} \sum_{k=0}^{n} C_{\tau,\tau}(k) \tag{26}$$

requires

$$C_{\tau,\tau}(n) \simeq \frac{\langle \tau \rangle^2}{2\sqrt{\pi}} \left(\frac{n_d}{n}\right)^{1/2}, \tag{27}$$

as displayed in Fig. 4(b).

In conclusion, subdiffusion in a stochastic single file occurs not because the first moments of the collisional parameters are infinitely large, as assumed in the CTRW models, but rather because they are statistically autocorrelated in a very special way. Negative power-law tails of the velocity and/or the jump autocorrelation functions have been predicted, indeed, for other 1D systems, such as the Jepsen's gas [4,25] and files of interacting particles [26], and, much earlier, also for the diffusive dynamics of a concentrated lattice gas in 3D [27]. Note, however, that *both conditions* (25) and (27) are required to predict SF diffusion. Similar conclusions have been reached also in the continuous time representation [16].

[1] B. Alberts *et al.*, *Molecular Biology of the Cell* (Garland, New York, 1994); J. Kärger and D. M. Ruthven, *Diffusion in Zeolites and Other Microporous Solids* (Wiley, New York, 1992).

[2] S. Savel'ev, F. Marchesoni, and F. Nori, Phys. Rev. Lett. **91**, 010601 (2003); **92**, 160602 (2004); S. Savel'ev *et al.*, Phys. Rev. E **74**, 021119 (2006).

[3] T. E. Harris, J. Appl. Probab. **2**, 323 (1965); D. G. Levitt, Phys. Rev. A **8**, 3050 (1973); J. K. Percus, *ibid.* **9**, 557 (1974).

[4] D. W. Jepsen, J. Math. Phys. **6**, 405 (1965); J. L. Lebowitz and J. K. Percus, Phys. Rev. **155**, 122 (1967).

[5] K. Hahn and J. Kärger, J. Phys. A **28**, 3061 (1995); K. Hahn, J. Kärger, and V. Kukla, Phys. Rev. Lett. **76**, 2762 (1996).

[6] K. Hahn and J. Kärger, J. Chem. Phys. **100**, 316 (1996).

[7] P. M. Richards, Phys. Rev. B **16**, 1393 (1977); H. van Beijeren, K. W. Kehr, and R. Kutner, *ibid.* **28**, 5711 (1983); J. Kärger *et al.*, J. Catal. **136**, 283 (1992); D. S. Sholl and K. A. Fichthorn, Phys. Rev. E **55**, 7753 (1997).

[8] P. Demontis *et al.*, J. Chem. Phys. **92**, 867 (1988); R. L. June, A. T. Bell, and D. N. Theodoru, *ibid.* **94**, 8232 (1990); **96**, 1051 (1992); U. Hong *et al.*, Zeolites **11**, 816 (1991).

[9] C. Lutz *et al.*, J. Phys.: Condens. Matter **16**, S4075 (2004); Q. H. Wei, C. Bechinger, and P. Leiderer, Science **287**, 625 (2000); C. Lutz, M. Kollmann, and C. Bechinger, Phys. Rev. Lett. **93**, 026001 (2004).

[10] H. L. Tepper *et al.*, J. Chem. Phys. **110**, 11511 (1999); K. K. Mon and J. K. Percus, J. Chem. Phys. **117**, 2289 (2002); K. K. Mon, J. K. Percus, and J. Yan, Mol. Simul. **29**, 721 (2003); M. Kollmann, Phys. Rev. Lett. **90**, 180602 (2003).

[11] J. W. M. Frenken, and J. F. van der Veen, Phys. Rev. Lett. **54**, 134 (1985); B. Pluis *et al.*, Phys. Rev. Lett. **59**, 2678 (1987); D. C. Senft and G. Ehrlich, *ibid.* **74**, 294 (1995); T. R. Linderoth *et al.*, Phys. Rev. Lett. **78**, 4978 (1997).

[12] P. Fulde, L. Pietronero, W. R. Schneider, and S. Strässler, Phys. Rev. Lett. **35**, 1776 (1975).
[13] L. P. Faucheux, G. Stolovitzky, and A. Libchaber, Phys. Rev. E **51**, 5239 (1995).
[14] S.-H. Lee, K. Ladavac, M. Polin, and D. G. Grier, Phys. Rev. Lett. **94**, 110601 (2005).
[15] A. Taloni and F. Marchesoni, Phys. Rev. Lett. **96**, 020601 (2006).
[16] F. Marchesoni and A. Taloni, Phys. Rev. Lett. **97**, 106101 (2006).
[17] H. van Beijeren, K. W. Kehr, and R. Kutner, Phys. Rev. B **28**, 5711 (1983).
[18] S. Giusepponi and F. Marchesoni, Europhys. Lett. **36**, 36 (2003).
[19] R. Metzler and J. Klafter, Phys. Rep. **339**, 1 (2000).
[20] H. C. Fogedby, Phys. Rev. E **50**, 1657 (1994).
[21] H. Risken, *The Fokker-Planck Equation* (Springer, Berlin, 1984).
[22] A. Papoulis, *Probability, Random Variables, and Stochastic Processes* (McGraw-Hill, New York, 1991).
[23] S. O. Rice, Bell Syst. Tech. J. **23**, 282 (1944); **24**, 46 (1945).
[24] J. P. de Gennes, J. Chem. Phys. **55**, 572 (1971).
[25] V. Balakrishnan, I. Bena, and C. Van den Broeck, Phys. Rev. E **65**, 031102 (2002).
[26] S. Pal *et al.*, J. Chem. Phys. **116**, 5941 (2002).
[27] K. W. Kehr *et al.*, Phys. Rev. B **23**, 4931 (1981).